

Los Alamos National Laboratory is operated by the University of California for the United States Department of Energy under contract W-7405-ENG-36.

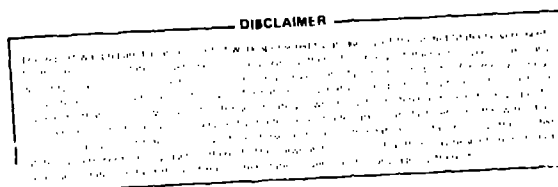
MASTER

LA-UR--82-2115

DE82 018113

TITLE: STATUS OF THE ICF PROGRAM AT LOS ALAMOS NATIONAL LABORATORY

AUTHOR(S): Stephen D. Rockwood



SUBMITTED TO: IAEA, 9th International Conference on Plasma Physics
and Controlled Nuclear Fusion Research, Baltimore, MD,
1-8 September 1982

gl
DISTRIBUTION OF THIS DOCUMENT IS UNLIMITED

By acceptance of this article, the publisher recognizes that the U.S. Government retains a nonexclusive, royalty-free license to publish or reproduce the published form of this contribution, or to allow others to do so, for U.S. Government purposes.

The Los Alamos National Laboratory requests that the publisher identify this article as work performed under the auspices of the U.S. Department of Energy.

Los Alamos Los Alamos National Laboratory
Los Alamos, New Mexico 87545

THE STATUS OF LASER FUSION RESEARCH
AT LOS ALAMOS NATIONAL LABORATORY

Abstract

The basic concept of achieving efficient thermonuclear fusion has been proven conclusively in nuclear weapons. The fundamental issue for inertial confinement fusion (ICF) is, how small can the fuel mass be?

The ICF program has two long-term goals. The first is to provide a laboratory capability for studying weapon physics. The attainment of this goal is not represented by any one event. Rather, benefits to the weapons program are being accrued continuously with greater understanding and improved diagnostics of materials under the extreme conditions of density and temperature similar to those achieved in nuclear explosions. The second goal is to provide a controllable source of fusion energy. This goal will be much more difficult to attain and not only requires the achievement of fusion in the laboratory but also a demonstration of engineering feasibility.

In the Los Alamos program we are emphasizing the testing of targets uniquely designed for drive with the carbon dioxide (CO₂) laser. The two major facilities for this study are the eight-beam Helios system and the Antares laser system. Some recent results to be discussed demonstrate the dominant effect of self-generated magnetic fields in controlling energy transport by hot electrons. An understanding of this physics may permit the design of targets for CO₂ that are self-shielding in terms of hot electron preheat.

Another consequence of the magnetic insulation is efficient energy conversion to ion motion. This occurs over a much larger surface than originally irradiated by the laser with in excess of 50 percent of the absorbed energy converted to ion motion in some experiments.

1. Introduction

The inertial fusion program at Los Alamos has stressed the use of the CO₂ laser for the goals of providing a laboratory capability for studying weapon physics and ultimately providing a controllable source of fusion energy. In this endeavor the CO₂ laser is recognized to have many desirable attributes as an operational laser system and could provide the repetition rate needed for energy applications. It is also recognized that the longer wavelength radiation of this laser produces hot electrons upon interaction with the plasma that must be dealt with by appropriate target designs. The majority of this paper will discuss a portion of the current knowledge and plans for CO₂ laser targets.

2. Background

When considering the prospects for success with ICF one must acknowledge that the basic concept of achieving efficient thermonuclear fusion has been proven conclusively in nuclear weapons. The fundamental issue for inertial fusion is, how small can the fuel mass be and still permit successful ignition and burn?

The achievement of efficient thermonuclear burn (TMB) requires attaining a constant value for the product of fuel density, ρ , and fuel volume radius, R . It then follows that to keep $\rho R = \text{constant}$ as the fuel mass, M , is decreased, the compressed density must increase as

$$\rho \approx 1/\sqrt{M} . \quad (1)$$

From this simple relationship some of the problems of scaling to small fuel masses are observed. The smaller the driver energy, the smaller the fuel mass that can be heated to ignition conditions; and the smaller the fuel mass, the better the target must be fabricated and illuminated to achieve implosion symmetry adequate to produce the required ρ .

The relationship between ρ and M from Eq. (1) is reproduced graphically in Fig. 1 for a $\rho R = 1 \text{ gm/cm}^2$. Also displayed in Fig. 1 are representative results for compression with $1 \text{ }\mu\text{m}$ and $10 \text{ }\mu\text{m}$ lasers. If these results represent the best possible compressions, then one observes very large increases in driver energy are required. This is not the preferred path for ICF.

Instead, one observes that the economic and program leverage is contained in the target physics. Present performance is far from optimum in approaching theoretical limits on compression. The major thrust of the program during the next several years will be in achieving greater compression and less preheat to move on a performance trajectory as indicated in Fig. 1. The target physics issues that are of greatest importance are: fusion ignition criteria, energy transport, implosion stability and materials properties.

3. The CO₂ Program

In the Los Alamos program the present facility for investigating target physics is the eight-beam Helios CO₂ laser. The operation of this laser has become very routine with an average of over 5 target shots per day in the 5 to 6 kJ energy range. This large rate of data production has allowed the establishment of good statistical averages for many parameters of interest to target design. Three important results for target design that have been investigated during the last year are: the dependence of absorption on laser intensity, the controlling mechanisms for electron energy transport, and the energy conversion processes in CO₂ laser irradiated targets. Each of these results will be discussed in turn.

Previous studies of laser-target interactions for laser radiation of $1\text{ }\mu\text{m}$ and shorter have shown a general decrease in the absorption as the laser intensity is increased.⁽¹⁾ For $10\text{ }\mu\text{m}$ radiation the absorption is always found to be in the range of 25 to 30 percent independent of laser intensity for values up to about 10^{15} W/cm^2 . Recent studies with Helios have extended the intensity range to 10^{16} W/cm^2 and a dramatic increase in absorption is observed. Some of this data is shown in Fig. 2 (solid line) along with confirming calculations from the plasma simulation code WAVE.⁽²⁾ The calculations predict absorption of 60 percent at $2 \times 10^{16}\text{ W/cm}^2$.

The precise nature of the plasma dynamics that lead to the higher absorption is not fully understood. However, two general observations are pertinent. The absorption increases as the electrons become relativistic. That is, when $kT_{\text{hot}}/m_0c^2 \sim 1$ where m_0 is the electron rest mass and T_{hot} the superthermal electron temperature in the plasma. For plasmas irradiated by CO_2 lasers at 10^{16} W/cm^2 T_{hot} is in the range of 200 keV.⁽³⁾ Secondly, when the electron motion becomes relativistic the critical surface, as observed in the plasma simulation codes, becomes highly structured on a fine spatial scale. This spatial structure produces a much larger surface area for absorption of the radiation. Since the onset of increased absorption is believed to be determined by the parameter kT_{hot}/m_0c^2 , and kT_{hot} is known to scale as $I\lambda^2$, one would expect the absorption to increase for other lasers when the product of their wavelength and intensity is of the order $I\lambda^2 \approx 10^{18}\text{ W-}\mu\text{m}^2/\text{cm}^2$.⁽⁴⁾ Some recent results with $1\text{ }\mu\text{m}$ lasers seem to confirm the general nature of this absorption-rise onset but at a lower value of $I\lambda^2$ than expected from the CO_2 results.⁽⁵⁾

The energetic benefits of the increased absorption just described are only realized at the expense of creating target design problems because of the hot electrons generated at high intensities. It is in regard to this problem that the new understanding of hot electron transport physics is so important. Recent experiments and fully self-consistent calculations have shown the dominant effect that self-generated magnetic fields play in electron transport.^(6,7)

The creation of self-generated magnetic fields in the corona of laser irradiated targets is well known.⁽⁸⁾ Recent calculations confirm that, for high intensity CO_2 laser irradiation, the magnetic fields are of sufficient strength ($\approx 1\text{ MG}$) to severely inhibit axial transport of the hot electrons and promote rapid lateral transport away from the laser focal spot.⁽⁷⁾ This model correlates a wide variety of previous transport experiments where non-diffusive behavior of the electrons was observed.

An intuitive understanding of the process is developed by viewing the coronal physics as described in Fig. 3. An initially-rapid escape of hot electrons from the laser focal

spot creates an electric field as indicated. This electric field has a large gradient at the edge of the laser focal spot support by the electron temperature gradient. A simple line integral of $\oint \mathbf{E} \cdot d\mathbf{l}$ around a closed path at the edge of the laser spot is then seen to have a non-zero value which gives rise to a finite value for dB/dt from Faraday's Law. The strong magnetic field generation is thus expected at the edge of the laser spot and is proportional to $\nabla \times \mathbf{E} \sim (\partial n / \partial z)(\partial T / \partial r)$ where n is the plasma density, T the electron temperature, z the coordinate normal to the target, and r the coordinate parallel to the target plane. For CO_2 laser driven targets these gradients may be very large due to the strong profile modification in n and the large values of T_{hot} .

For high intensity irradiation the B field becomes large enough to trap high energy electrons in the corona and prevent them from returning to the target. The electrons then move laterally away from the focal spot in an $\mathbf{E} \times \mathbf{B}$ driven drift. The velocity of this drift is estimated to be

$$v_d \approx \left(\frac{c \sqrt{4\pi}}{\omega_{pe} L_n} \right) v_e \quad (2)$$

where v_e is the hot electron thermal speed, ω_{pe} the electron plasma frequency, and L_n the density gradient scale length normal to the target.⁽⁹⁾

While the energetic electrons that escape the target are trapped in the corona by the electric and magnetic fields the low energy electrons are confined to local deposition near the laser focal spot. Thus, one observes an axial transport that is representative of colder than average electrons, or the appearance of inhibited axial transport, coupled with rapid lateral transport of electron energy. The magnetic insulation is maintained until interrupted by interference with fields from neighboring focal spots or fringing fields at the edge of targets.

The experiments reported in Ref. (6) have pursued the effects of beam irradiation geometry on electron deposition in a variety of planar, cylindrical or spherical targets. In all cases the results were qualitatively consistent with the predictions of the magnetic field model. A typical result is shown in Fig. 4 for cylindrical targets. The picture is obtained from K_α x-ray emission from a Ni layer in the target that serves as a monitor of hot electron deposition. The target was a cylinder 500 μm in diameter and irradiated by four beams of Helios evenly spaced upon the surface. Strong electron deposition is observed at the laser focal spot and at the locus of points equidistant from the laser focal spots where destructive interference of the magnetic fields can occur. Deposition is also observed on the cylinder edges due to fringing field effects. Of special significance for preventing electron preheat of fusion targets is the lack of electron deposition over a relatively large area adjacent to the laser focal spots and the ability to control this area

through target irradiation geometry. The magnetic insulation is effective over an area many times larger than the focal spot area.

Because of the charge separation maintained by the magnetic insulation, the area adjacent to the laser focal spot becomes an efficient ion diode. Previous studies have indicated conversion of incident CO₂ laser energy into fast ion blow-off from the target.⁽¹⁰⁾ Recent studies have extended this study to higher intensities.⁽²⁾ These results on conversion efficiency are shown in Fig. 2 (dashed line). It is observed that over 65 percent of the absorbed laser energy is converted to fast ion energy. Moreover, since the absorption at high intensities is as high as 60 percent it has been possible to convert up to 40 percent of the incident laser energy into the single mode of ion kinetic energy. Previous studies have shown for protons that this ion distribution is centered around 1 MeV.⁽¹⁰⁾

4. Future Directions

Thus the current thinking on CO₂ laser targets is to capitalize on all of the above observations by creating ions to drive a target while isolating the hot electrons by magnetic and electrostatic fields. In this design the laser beams are tightly focused onto an ion converter. The tight focus leads to efficient absorption and ion generation as described above. The unwanted hot electrons are confined to the sheath thickness ($\sim 10 \mu\text{m}$) of the converter surface by the self-generated magnetic fields. These hot electrons will generally move laterally along the converter surface and deposit at weak field points along the converter edge or on the side away from the laser. This effectively mitigates the preheat problem in the fuel region. The energy is then efficiently transmitted to the fuel capsule by the ion beam that is originally leaving at the surface normal of the converter.

Recent experiments on the focusability of the ions emitted from such surfaces have shown encouraging results in a geometry as shown in Fig. 6. It is found that approximately 70 percent of the ion energy is contained in a 15° cone angle. In fact, using the measured conversion efficiency from laser radiation to ions, the known pulse length, and the measured divergence of the ion beam one can calculate a brightness of about 50 TW/cm²/sr achieved in Helios experiments. This is the brightest ion beam source known. Experiments are continuing on these targets. The major thrust of the experiments is parameterization of the ion transport and focusability.

Another critical set of experiments will be the determination of the hot electron preheat levels in the fuel region. It is generally believed that the hot electrons will be effectively shielded by electrostatic and magnetic forces until the fast ions traverse the gap and cause a shorting of the diode. If this shorting time is longer than the laser pulse length the hot electron preheat problem may be effectively mitigated.

Taken in concert, the new discoveries described here have opened a variety of new options for designers to follow in the creation of targets suited to the carbon dioxide laser. During the coming year we are anxious to try these concepts at the higher energy levels available from Antares and assess their potential for future applications satisfying the goals of the ICF program.

Acknowledgement

Work performed by members of the Inertial Fusion Program at the Los Alamos National Laboratory under the auspices of the US Department of Energy.

References

- (1) NISHIMURA, H., et al., Experimental study of wavelength dependences of laser-plasma coupling, transport, and ablation processes, Phys. Rev. A 23 (1981) 2011.
- (2) KEPHART, J.F., et al., Measurement of absorption and fast ion loss in high energy experiments at Helios, Anomalous Absorption Conf. Proc., Santa Fe, New Mexico, May 1982. Calculation by D. W. FORSLUND (private communication).
- (3) PRIEDHORSKY, W., et al., Hard x-ray measurements of 10.6 μm laser-irradiated targets, Phys. Rev. Lett. 47 (1981) 1661.
- (4) TAN, T.H., MCCALL, G.H., WILLIAMS, A.H., Determination of laser intensity and hot electron temperature from fastest ion velocity measurement on laser produced plasma, submitted to Phys. of Fluids.
- (5) HAMA, H., et al., Intensity dependence of classical and collective absorption processes in laser produced plasmas at 1.053 μm and 0.527 μm , IEEE Trans. Plasma Sci. PS-10 (1982) 55.
- (6) YATES, M.A., et al., Experimental evidence for self-generated magnetic fields and remote energy deposition in laser irradiated targets, submitted to Phys. Rev. Lett.
- (7) FORSLUND, D.W., BRACKBILL, J.U., Magnetic field induced surface transport on laser irradiated foils, Phys. Rev. Lett. 48 (1982) 1614.
- (8) STAMPER, J., RIPIN, B.H., Faraday-rotation measurements of megagauss magnetic fields in laser-produced plasmas, Phys. Rev. Lett. 34 (1975) 138.
- (9) FORSLUND, D.W., (private communication).
- (10) EHRLER, A.W., High energy ions from a CO₂ laser produced plasma, J. App. Phys. 46 (1975) 2464.

- Fig. 1 Maintaining a constant product of fuel density and radius as the target mass decreases dictates that the compression increase.
- Fig. 2 The absorption of 10.6 μm light is observed to increase in experiments (solid line) and calculations (squares) as the laser intensity is increased. It is also observed that most of the energy goes into fast ions (dashed line).
- Fig. 3 Schematic representation of the interaction of the electrons with the self-generated electric and magnetic fields. These fields act as an energy selector of electrons striking the target and dominate all aspects of the transport at high laser intensities.
- Fig. 4 X-ray photograph of cylindrical targets illuminated by four beams of the Helios laser. The targets were 25- μm thick Ni tubes. The x-rays show the location of the electron deposition. The upper image is filtered with iron foil which passes 5 to 7 keV x rays. The second image is filtered into beryllium foil passing all x rays above 1 keV. The bottom image is filtered by Ni foil passing x rays from 6 to 8 keV. The interesting feature is the lack of deposition adjacent to the laser spot but intense deposition along a line equidistant to the focal position.
- Fig. 5 Schematic of the experimental arrangement used to measure the brightness of the ion diode created by high intensity laser illumination.

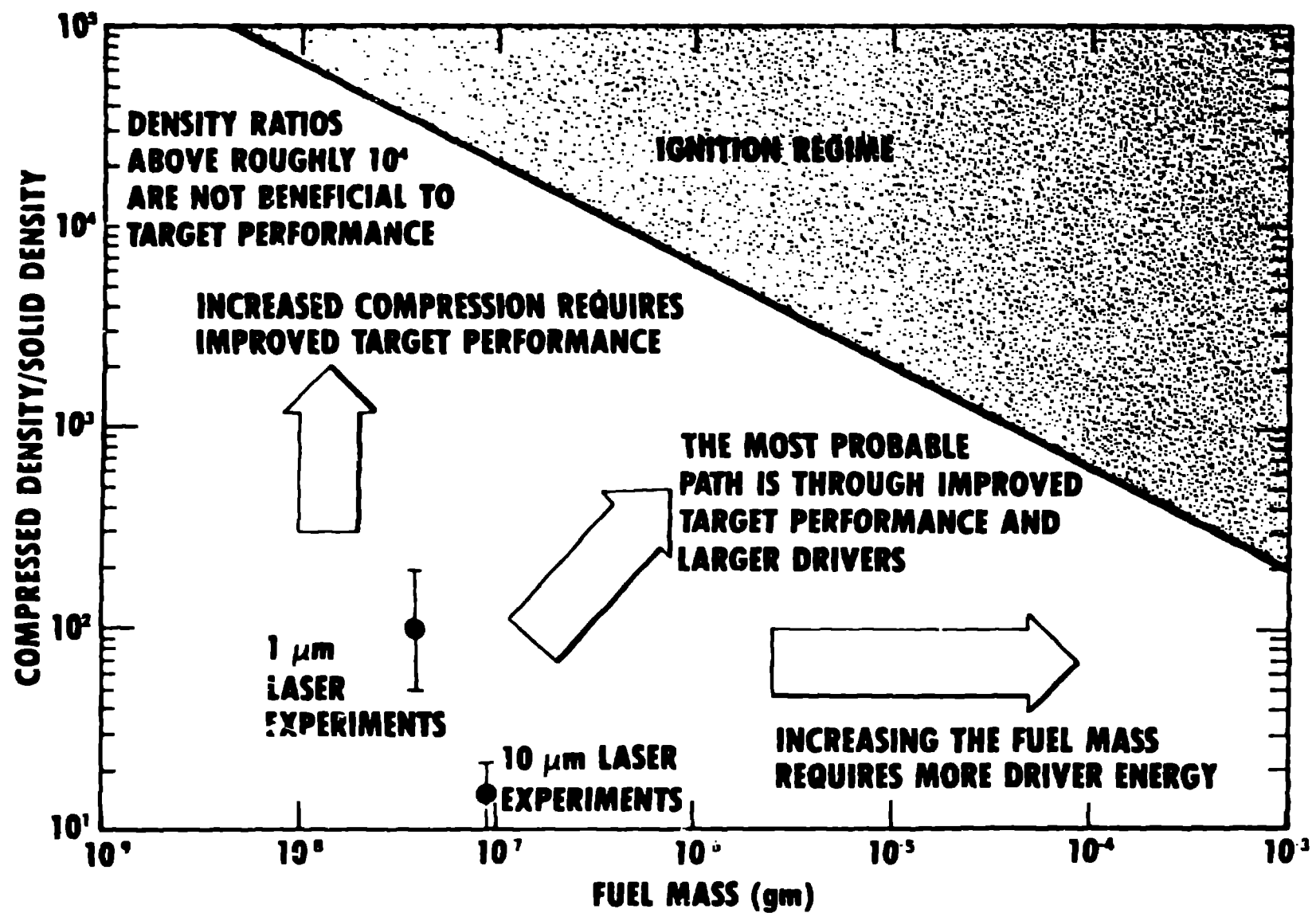


Fig. 1. Maintaining a constant product of fuel density and radius as the target mass decreases dictates that the compression increase.

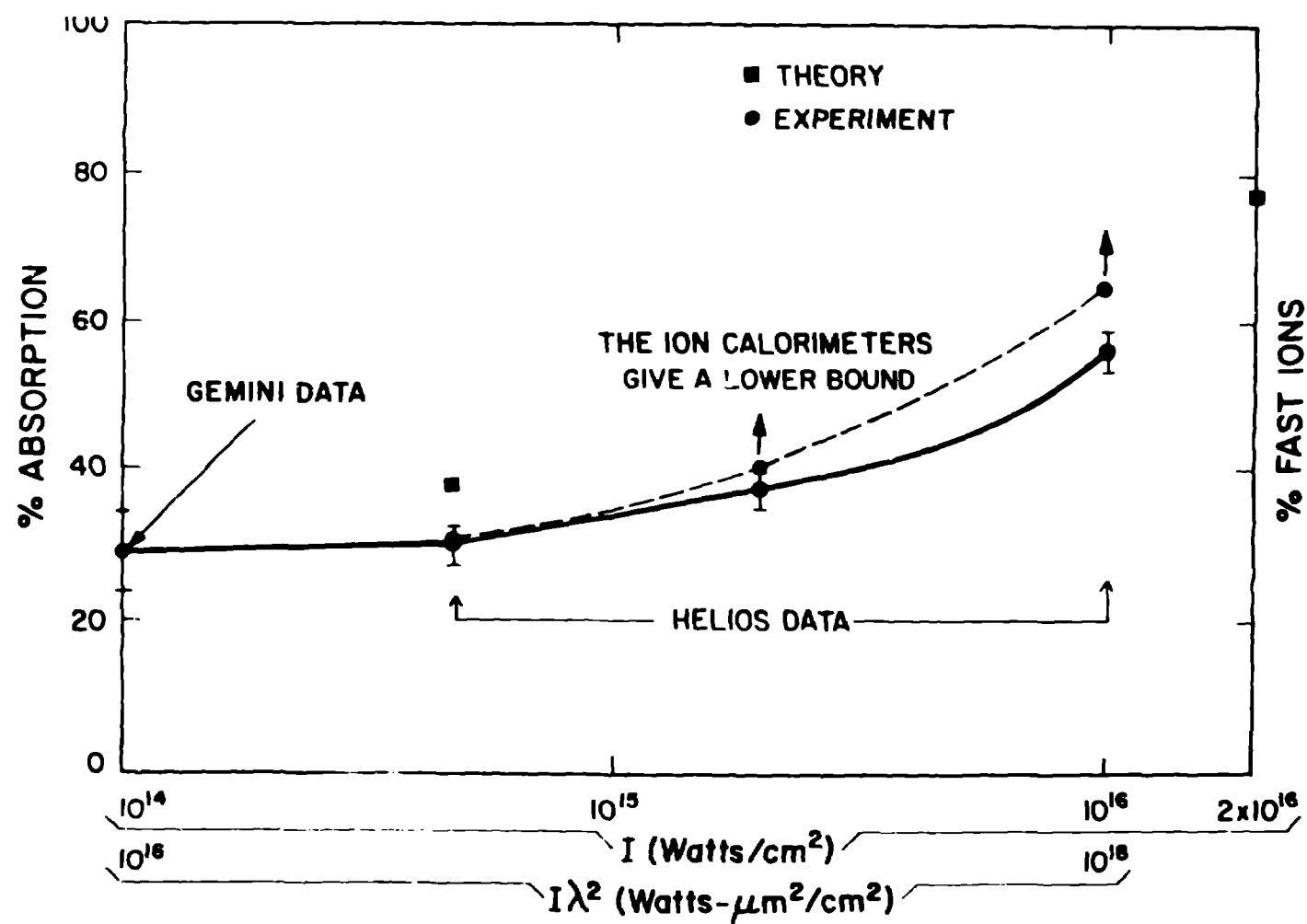


Fig. 2. The absorption of 10.6 μ m light is observed to increase in experiments (solid line) and calculations (squares) as the laser intensity is increased. It is also observed that most of the energy goes into fast ions (dashed line).

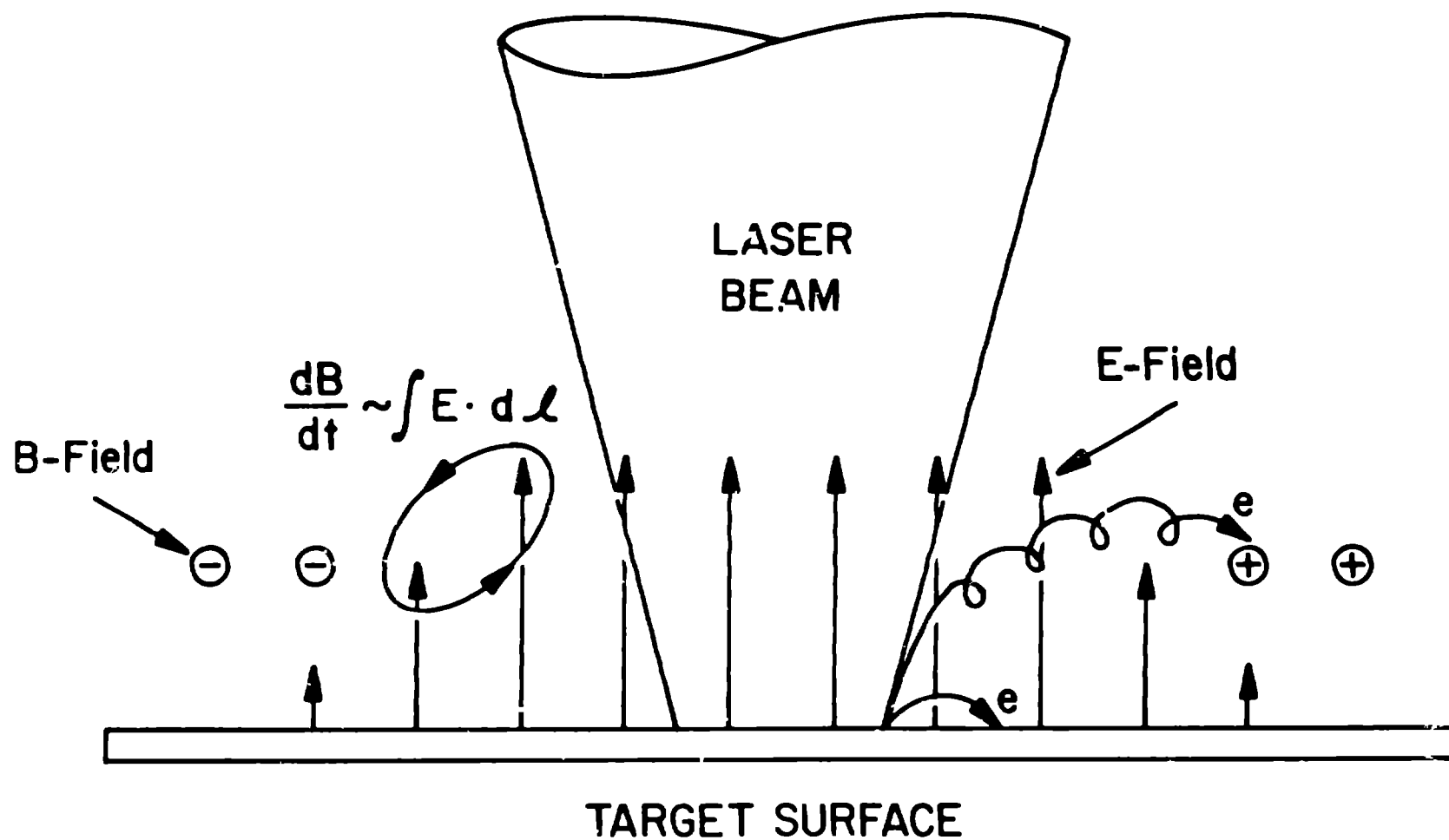


Fig. 3. Schematic representation of the interaction of the electrons with the self-generated electric and magnetic fields. These fields act as an energy selector of electrons striking the target and dominate all aspects of the transport at high laser intensities.

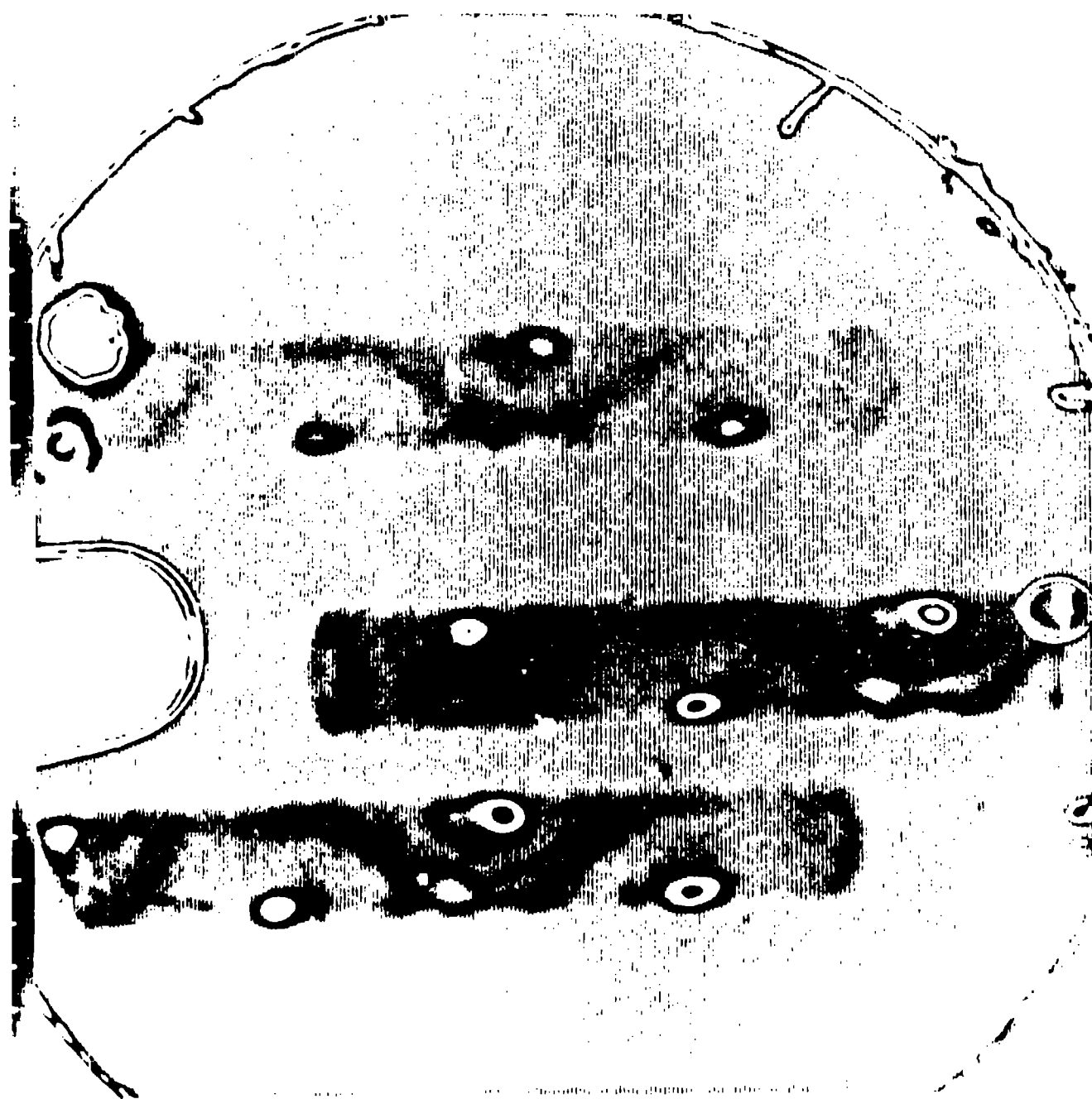


Fig. 4. X-ray photograph of cylindrical targets illuminated by four beams of the Helios laser. The targets were 25- μ m thick Ni tubes. The x rays show the location of the electron deposition. The upper image is filtered with iron foil which passes 5 to 7 keV x rays. The second image is filtered into beryllium foil passing all x rays above 1 keV. The bottom image is filtered by Ni foil passing x rays from 6 to 8 keV. The interesting feature is the lack of deposition adjacent to the laser spot but intense deposition along a line equidistant to the focal position.

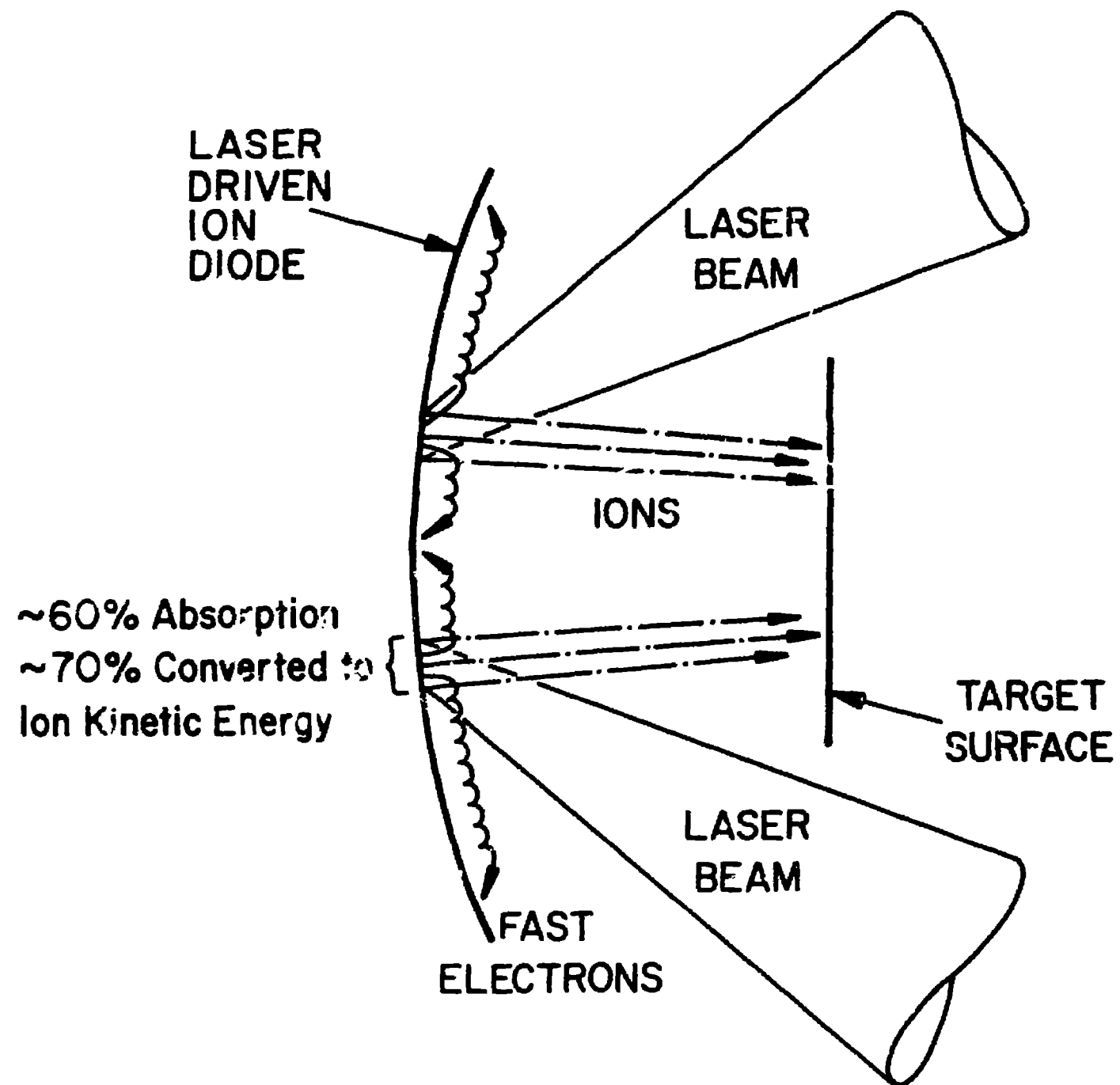


Fig. 5. Schematic of the experimental arrangement used to measure the brightness of the ion diode created by high intensity laser illumination.